

## Detection of Very-High-Energy Gamma-Ray Emission from the Gamma-Ray Binary LS5039

Hongkui Lv,<sup>a,b</sup> Huihai He,<sup>a,b,c</sup> Mariam Hasan,<sup>a,c</sup> Cong Li,<sup>a,b,\*</sup> Qinyi Cheng<sup>a,c</sup> and Shicong Hu<sup>a,b</sup>

<sup>a</sup>State Key Laboratory of Particle Astrophysics, Institute of High Energy Physics, Chinese Academy of Sciences, Beijing 100049, China

<sup>b</sup>Tianfu Cosmic Ray Research Center, Chengdu, Sichuan, China

<sup>c</sup>University of Chinese Academy of Sciences, Beijing 100049, China

E-mail: [lvhk@ihep.ac.cn](mailto:lvhk@ihep.ac.cn)

Binary systems are potential very-high-energy (VHE) gamma-ray emitters, however, the VHE gamma-ray emission mechanism of these systems remains poorly understood. Recent observational results from H.E.S.S. and HAWC on the gamma-ray binary LS 5039 suggest that the binary system can efficiently accelerate particle, making it a possible candidate for the origin of PeV cosmic rays in the Milky Way. In this study, we search for VHE gamma-rays above  $\sim 10$  TeV from the LS 5039, which consists of a massive star with a mass of  $23 M_{\odot}$  and an unknown compact object, using LHAASO data. Leveraging the high sensitivity of the LHAASO experiment in VHE gamma-ray observations, we have confirmed the VHE gamma-ray emission from LS 5039 up to 100 TeV, with its spectrum exhibiting no discernible cutoff.

39th International Cosmic Ray Conference (ICRC2025)  
15–24 July 2025  
Geneva, Switzerland



**ICRC 2025**

The Astroparticle Physics Conference  
Geneva July 15-24, 2025

\*Speaker

## 1. Introduction

Gamma-ray binaries are composed of a stellar-mass compact object (pulsar or black hole) and a massive star typically with a mass of  $10 \sim 20 M_{\odot}$ . This class of sources offers a unique experimental environment, giving access to various vantage points or physical conditions on a regular timescale as the components revolve on their orbit. The first evidence of their existence is based on the detection of very-high-energy (VHE) gamma-rays from PSR B1259-63, observed by the H.E.S.S. around 2005. Subsequently, several other instances have been observed by ground-based VHE gamma-ray observation experiments around the mid-2000s, including LS 5039 [1], LSI+61°303 [2] and so on. Until now, a dozen gamma-ray binaries have been reported, mostly identified by imaging air Cherenkov telescopes.

Extensive studies have been conducted to investigate the potential characteristics of gamma-ray binaries from multiwavelength observations [3]. Notably, these sources exhibit orbital modulations across all wavelengths and share many similar properties in terms of spectral features. They consistently display radio emission, modest X-ray fluxes, and hard X-ray spectra with a typical index of 1.5 to 2, extending to high energies or VHE. In terms of VHE emission, all counterparts are point-like, with a typical expansion within  $0.1^{\circ}$ . Spectral variability is observed according to the orbital phase, ranging from inferior conjunction (INFC) to superior conjunction (SUPC).

Gamma-ray binary systems are believed to have the ability to efficiently accelerate particles, potentially serving as PeV accelerators [4]. However, the VHE gamma-ray emission mechanism of these systems remains largely unknown. The emission has been suggested to be generated by the accretion energy released in the form of relativistic jets (named microquasar) or by the rotational energy released as pulsar winds. The origin of VHE gamma-ray is also highly debated either by the decay of neutral pions via hadronic interactions or by the inverse Compton scattering of optical to UV photons from the star by relativistic electrons.

The VHE gamma-ray emission from the gamma-ray binary LS 5039 was initially identified by H.E.S.S. in 2005 [1]. This binary system hosts a massive star with a mass of  $23 M_{\odot}$  and a radius of  $9.3 R_{\odot}$ , assuming the compact object is a neutron star of  $1.4 M_{\odot}$ . It has an orbital period of approximately 3.9 days and an eccentricity of around 0.35, as shown in Figure 1. Recently, HAWC also reported significant VHE gamma-ray emission coinciding with the position of LS 5039, confirming flux modulation with orbital phase (at a  $4.7\sigma$  confidence level) in the energy range of 2 TeV to 118 TeV. The spectrum extends beyond 100 TeV without a cutoff, making LS 5039 a possible candidate for the origin of PeV cosmic rays in the Milky Way [5]. Leveraging the high sensitivity of LHAASO for VHE gamma-ray observation above  $\sim 30$  TeV, we aim to identify the VHE gamma-ray emission from LS 5039, particularly the gamma-ray above 100 TeV, and investigate its spectral characteristics.

## 2. The LHAASO Experiment

LHAASO is located at Haizi Mountain (4410 meters above sea level in Sichuan, China). It consists of three sub-arrays: the square kilometer array (KM2A), a 78,000 m<sup>2</sup> water Cherenkov detector array (WCDA), and 18 wide-field air Cherenkov/fluorescence telescope array (WFCTA). The KM2A consists of 5216 electromagnetic detectors (EDs) and 1188 muon detectors (MDs),

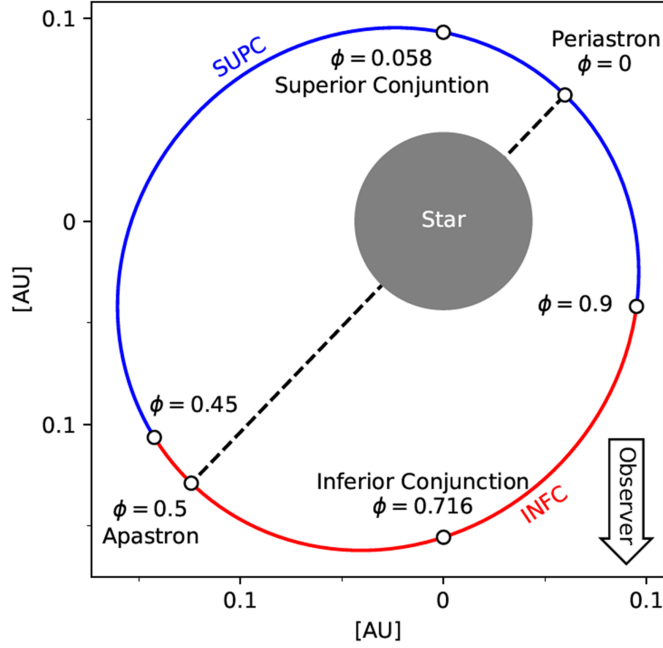


**Figure 1:** The orbital period of the LS 5039 system is approximately 3.9 days. The periastron, apastron, and conjunctions are indicated in the figure. The orbit is divided into two parts: INFC (ranging from  $0.45 < \phi < 0.9$ ) and SUPC (ranging from  $0.9 < \phi < 1$  and  $0 < \phi < 0.45$ ) [6].

covering an area of approximately  $1.3 \text{ km}^2$ . The EDs are designed to measure the number density and arrival times of charged particles within EASs produced by primary particles. The MDs are particularly useful for discriminating between gamma-ray events and cosmic ray backgrounds, as gamma-ray induced showers are muon-poor, while cosmic ray induced showers are muon-rich. A comprehensive performance study of the WCDA and KM2A detectors, based on Monte Carlo simulations and observations of the Crab Nebula, is presented in [7, 8].

The WCDA data used in this analysis were collected from 5th March 2021 to 31st July 2024, and the KM2A data used were collected from 27th December 2019 to 31st December 2024. The WCDA covers an observation energy range from  $\sim 1 \text{ TeV}$  to several tens of TeV, while the KM2A covers an observation energy range of greater than 25 TeV. Detailed descriptions of data reconstruction methods are provided in [7, 8].

### 3. Analytical methods

After data reconstruction, the sky map in celestial coordinates is divided into a grid of  $0.1^\circ \times 0.1^\circ$  pixels. Each pixel is filled with the number of detected events based on their reconstructed arrival directions. The "direct integration method" is used to estimate the number of cosmic-ray background events in each grid.

In this work, the data from KM2A and WCDA are analyzed separately, but the analysis methods are identical. The significance of the source is evaluated using a test statistic, defined as  $TS = \frac{\mathcal{L}_{s+b}}{\mathcal{L}_b}$ , where  $\mathcal{L}_{s+b}$  or  $\mathcal{L}_b$  is obtained by comparing the observed event counts with the expected counts.

For  $\mathcal{L}_b$ , the expected counts are derived from the background maps extracted from the data. For  $\mathcal{L}_s$ , the expected counts correspond to the signal contribution of the source plus the background hypothesis. In the significance test, the LS 5039 signal model is set as a point source model with a fixed position, and the only free parameter is the total number of events. The value of  $TS$  follows a  $\chi^2$  distribution with the number of free parameters in the signal model. Therefore,  $\pm\sqrt{TS}$  can be taken as the significance of the observed results.

For the determination of the morphology and flux of the source, we use a 3D Likelihood method. The first step is to build the morphology and spectrum of each source in the ROI. In this work, the spectrum of LS 5039 is assumed to be a simple power-law distribution, and the morphology is set as a point source model. Then the parameters of each source model are estimated using maximum likelihood estimation.

#### 4. Results

Using the 3D Likelihood method described in section 3, we list all the sources observed by WCDA and KM2A in the ROI region in Table 1 and Table 2. It should be noted that the morphological template used to fit the 6 TeV to 25 TeV data includes one additional Gaussian extended source (J1824-1400) compared to the >25 TeV analysis. This is because, in the KM2A data analysis, the hypothesis of four sources did not show a significant improvement in detection significance over the three sources model. Statistically, the KM2A observations in this region favor the hypothesis of three sources.

Name	R.A.(°)	Dec.(°)	Extension(°)	$F_0$ @ 10 TeV ( $\text{TeV}^{-1}\text{cm}^{-1}\text{s}^{-1}$ )	Index
J1825-1256	276.57±0.02	-12.96±0.03	0.15±0.02	(1.16±0.10)e <sup>-14</sup>	2.15±0.09
J1825-1337	276.55±0.01	-13.65±0.02	0.24±0.01	(7.07±0.22)e <sup>-14</sup>	2.46±0.05
J1824-1400	276.49±0.06	-14.36±0.09	0.72±0.08	(5.44±0.43)e <sup>-14</sup>	3.45±0.45
Point source (LS5039)	276.63±0.06	-14.44±0.10	/	(6.36±1.87)e <sup>-15</sup>	3.23±0.54

**Table 1:** List of fit results around LS 5039 using WCDA data (6 TeV to 25 TeV). The spectra of the sources are assumed to follow a power-law distribution. The morphology of the sources is modeled as three Gaussian sources and one point source (LS 5039).

Name	R.A.(°)	Dec.(°)	Extension(°)	$F_0$ @ 10 TeV ( $\text{TeV}^{-1}\text{cm}^{-1}\text{s}^{-1}$ )	Index	$E_{cut}$ (TeV)
J1825-1256	276.50±0.02	-12.94±0.03	0.08±0.04	(9.89±0.67)e <sup>-14</sup>	3.46±0.10	/
J1825-1337	276.50±0.01	-13.62±0.02	0.19±0.01	(11.25±0.36)e <sup>-14</sup>	2.61±0.15	194.1±48.1
Point source (LS5039)	276.68±0.06	-14.64±0.07	/	(6.43±1.11)e <sup>-14</sup>	3.89±0.26	/

**Table 2:** List of fit results around LS 5039 using KM2A data (above 25 TeV). The spectra of the sources are assumed to follow a power-law distribution or a power-law with an exponential cutoff. The morphology of the sources is modeled as two Gaussian sources and one point source (LS 5039).

The significance map of gamma-ray emission around LS 5039, after subtraction of other sources, are shown in Figure 2. In the energy ranges of 6 TeV to 25 TeV and above 25 TeV, gamma-ray signals around LS 5039 were detected with statistical significances of  $4.1\sigma$  and  $7.0\sigma$ ,

respectively. The position of the  $>25$  TeV gamma-ray point source in the equatorial coordinate is  $(299.68^\circ \pm 0.06^\circ, -14.64^\circ \pm 0.07^\circ)$ . This position deviates by  $0.24^\circ$  from the position of LS 5039 observed by H.E.S.S..

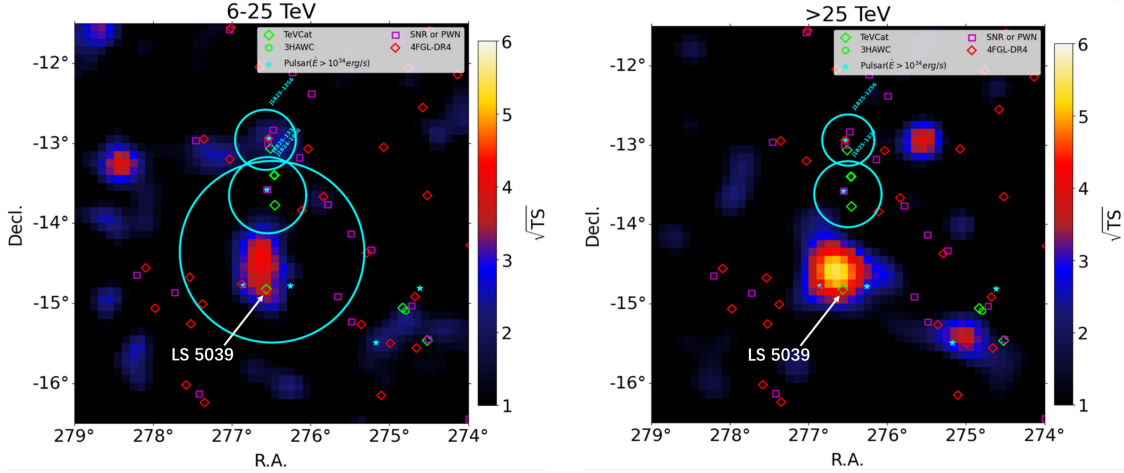


**Figure 2:** The significance map of gamma-ray emission around LS 5039 after subtraction of background sources (Left: using WCDa data with energies in the range of 6 TeV to 25 TeV. Right: using KM2A data with energies above 25 TeV). The open circle shows the location of the background sources (J1825-1256, J1825-1337, and J1824-1400). The green rectangle marked by the white arrow, corresponds to the location of LS 5039 observed by H.E.S.S..

The spectral parameters of the point source differ between the energy ranges of 6 TeV to 25 TeV and  $>25$  TeV. This indicates that the spectrum does not follow a single power-law distribution across the entire detection energy range. The spectral energy distribution (SED) of the point source is shown in Figure 3. The SED observed by WCDa in the 6 TeV to 25 TeV energy band lie within the bounds of the inferior conjunction (INFC) and superior conjunction (SUPC) phase SED results observed by H.E.S.S. [9], providing evidence that the gamma-ray signal from the point source originates from LS 5039. Based on current observational data, the SED extends to 100 TeV without exhibiting a discernible cutoff. More complex spectral analysis requires joint analysis of WCDa and KM2A data, which will be discussed in a separate paper.

## 5. Conclusion

Using WCDa data with a live time of 1137 days and KM2A data with a live time of 1733 days, we have confirmed the presence of VHE gamma-ray emission from LS 5039 reaching energies up to 100 TeV, with no observed spectral cutoff. This indicates that LS 5039 possesses extremely powerful particle acceleration capabilities. In the future, as the LHAASO experiment accumulates more data, we will continue to analyze the phase-resolved VHE spectrum of LS 5039 and investigate whether significant orbital modulation exists above 100 TeV. This will contribute to a better understanding of the acceleration processes in binary systems.

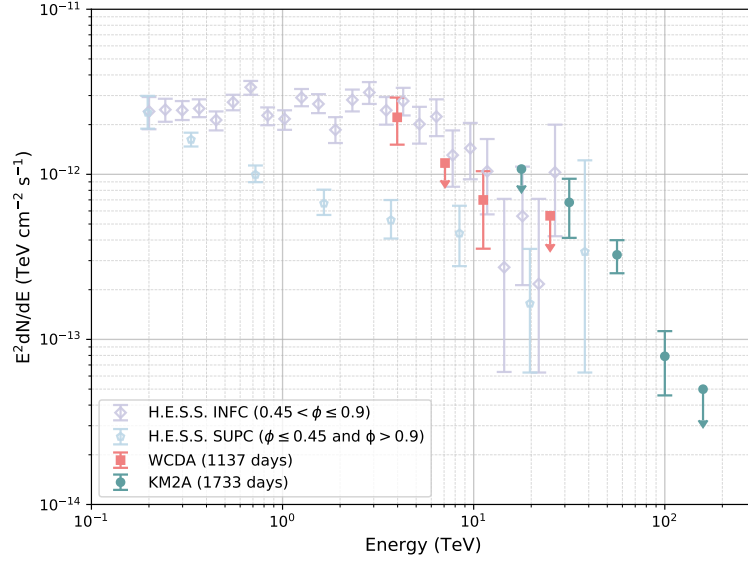


**Figure 3:** The spectral energy distribution (SED) of VHE gamma-ray around LS 5039 observed by WCDA and KM2A. The open green and open purple data points represent the H.E.S.S. measured spectral energy distributions of LS 5039 [9], during its inferior conjunction (INFC) and superior conjunction (SUPC) orbital phases, respectively.

## References

- [1] F. Aharonian, A.G. Akhperjanian et al., *Discovery of very high energy gamma rays associated with an x-ray binary*, *Science* **309** (2005) 746.
- [2] J. Albert, E. Aliu et al., *Variable very-high-energy gamma-ray emission from the microquasar ls i +61 303*, *Science* **312** (2006) 1771.
- [3] G. Dubus, *Gamma-ray binaries and related systems*, *The Astronomy and Astrophysics Review* **21** (2013) .
- [4] A. Bykov, A. Petrov et al., *Pev proton acceleration in gamma-ray binaries*, *Advances in Space Research* **74** (2024) 4276.
- [5] R. Alfaro, M. Araya et al., *Orbital modulation of gamma-rays beyond 100 tev from ls 5039*, 2025.
- [6] Huber, D., Kissmann, R. et al., *Relativistic fluid modelling of gamma-ray binaries - ii. application to ls 5039*, *AA* **649** (2021) A71.
- [7] F. Aharonian, Q. An et al., *Observation of the crab nebula with lhaaso-km2a a performance study*, *Chinese Physics C* **45** (2021) 025002.
- [8] F. Aharonian, Q. An et al., *Performance of lhaaso-wcda and observation of the crab nebula as a standard candle*, *Chinese Physics C* **45** (2021) 085002.

- [9] Aharonian, F., Akhperjanian, A. G. et al., *3.9 day orbital modulation in the tev  $\gamma$ -ray flux and spectrum from the x-ray binary ls 5039*, [AA 460 \(2006\) 743](#).